

Georisk: Assessment and Management of Risk for Engineered Systems and Geohazards

ISSN: 1749-9518 (Print) 1749-9526 (Online) Journal homepage: www.tandfonline.com/journals/ngrk20

Updated normalized load-settlement model for full-scale footings on granular soils

Shadi S. Najjar, Elie Shamma & Michel Saad

To cite this article: Shadi S. Najjar, Elie Shamma & Michel Saad (2014) Updated normalized load-settlement model for full-scale footings on granular soils, *Georisk: Assessment and Management of Risk for Engineered Systems and Geohazards*, 8:1, 63-80, DOI: [10.1080/17499518.2013.836419](https://doi.org/10.1080/17499518.2013.836419)

To link to this article: <https://doi.org/10.1080/17499518.2013.836419>



Published online: 03 Oct 2013.



Submit your article to this journal [↗](#)



Article views: 139



View related articles [↗](#)



View Crossmark data [↗](#)

Updated normalized load-settlement model for full-scale footings on granular soils

Shadi S. Najjar^{a*}, Elie Shammass^b and Michel Saad^a

^a*Department of Civil and Environmental Engineering, American University of Beirut, Beirut, Lebanon;* ^b*Department of Mechanical Engineering, American University of Beirut, Beirut, Lebanon*

(Received 26 April 2013; accepted 15 August 2013)

The design of spread footings on granular soils is generally governed by serviceability requirements. Recent studies have utilized databases of load tests to investigate the use of normalized load-settlement curves to model the behavior of footings on sands. A major limitation of available databases is that they are based primarily on data from plate load tests or footings that have an equivalent width smaller than 1.0 m. There is a need to confirm the applicability of these curves to footings of practical scale. The main objective of this paper is to update available normalized load-settlement curves using point measurements of settlement and load from full-scale footings. Bayesian techniques are employed in the updating process. Results indicate that the updated normalized load-settlement relationship is slightly more conservative but less uncertain than the current relationship. Results from an illustrative example involving serviceability limit state reliability analyses using footings with widths ranging from 1.5 to 3.0 m indicated that the updated relationship resulted in a slightly higher reliability level compared to the prior relationship.

Keywords: Bayesian methods; foundations; reliability analysis; limit state design; probability of failure

1. Introduction and background

Shallow foundations are generally designed to satisfy bearing capacity and settlement criteria. For granular soils (sands and gravel), if the bearing capacity of a foundation is ensured with an adequate margin of safety, the design of the foundation is governed largely by the requirement that foundation movements must be within limits that can be tolerated by the superstructure (Meyerhof 1965). As such, the efficient design of shallow foundations on granular soil is governed by the accuracy and reliability of current settlement prediction models.

Settlement prediction is subject to a considerable level of uncertainty. Natural deposits of granular soil are inherently variable, both laterally and vertically, with the variability differing from site to site. Based on an analysis of cases where more than one footing was present in a given site, Burland and Burbidge (1985) state that the measured settlements in a site generally lie between plus or minus 50% of the average value. In addition, soil characteristics affecting settlement are generally poorly defined as a result of limited spatial sampling and errors associated with the measurement techniques. Fenton, Griffiths, and Cavers (2005), Shahin, Jaksa, and Maier (2005), Akbas and Kulhawy (2009c), and Uzielli and Mayne (2012) studied the effect of spatial variability in soil properties on the reliability-based design of foundations on granular

soil. In these studies, spatial variability in soil properties was found to have a significant effect on both the total and differential settlements of footings on sands and thus on the serviceability limit state design of these foundations.

Uncertainties due to inherent variability in soil properties are amplified by uncertainties and limitations of currently available models for predicting settlement. Model uncertainty results from the simplified and empirical nature of models which generally rely on the Standard Penetration Test (SPT) or the Cone Penetration Test (CPT) for estimating the compressibility or stiffness of the soil. The empirical nature of such prediction methods represents their greatest disadvantage.

Settlements computed by different methods have been compared against measured settlements by several researchers (Jeyapalan and Boehm 1986; Tan and Duncan 1991; Berardi and Lancellotta 1991; Sivakugan and Johnson 2002; Akbas 2007). A common finding between all studies is that substantial scatter exists between measured and predicted settlements. For example, in Sivakugan and Johnson (2002), the average and coefficient of variation of the ratio of predicted to measured settlement are reported, respectively, as 3.52 and 0.89 for the Terzaghi and Peck (1967) method, 2.66 and 0.785 for the Schmertmann, Hartman, and Brown (1978) method, and 1.51 and 0.73 for the Burland and Burbidge (1985) method.

*Corresponding author. Email: sn06@aub.edu.lb

The average ratio of predicted to measured settlement for a given settlement prediction model is an indication of model accuracy and bias. On the other hand, the coefficient of variation in the ratio of predicted to measured settlement is an indication of the model uncertainty. The above statistics for the ratio of predicted to measured settlement indicate that traditional methods of settlement prediction lack accuracy and consistency.

Most traditional methods of settlement prediction for footings on granular soil do not address the expected nonlinearity in the load-settlement behavior. As a result, recent efforts in this field have attempted to study the overall load-settlement behavior of a foundation under load using various analytical and empirical models (Lutenegger and Adams 1998; Briaud 2007; Elfass, Norris, and Vilamaraj 2007) or using the observed behavior of well-documented footing tests which allows for an assessment of the overall generalized load-settlement behavior of footings (Akbas and Kulhawy 2009a; Uzielli and Mayne 2012).

Akbas and Kulhawy (2009a) assembled a database comprised of 167 axial compression tests with complete load-settlement curves for footings on soils ranging from silt to gravel. The database was used to evaluate the normalized load-settlement behavior of footings in granular soils. The normalization was conducted by dividing the settlement (s) by the footing width (B) and the force (Q) by the interpreted failure load (Q_{L2}), which is defined as the failure threshold which corresponds to the beginning of the final linear portion of the

load-settlement curve (Akbas and Kulhawy 2009a). The normalization was conducted to achieve a common load-settlement behavior for all the tests in the database.

To achieve this objective, Akbas and Kulhawy (2009a) approximated the normalized load-settlement curves measured for each load test in the database using a hyperbolic fitting model with two fitting parameters, a and b such that:

$$Q/Q_{L2} = \frac{s/B}{a(s/B) + b} \quad (1)$$

The parameters a and b were calculated using least squares regression. For the 125 cases analyzed (42 out of 167 test cases were not included in the analysis since the load tests in these cases were terminated at small settlements), results indicated averages and coefficients of variation of 0.7 and 0.22 (for parameter a) and 1.77 and 0.54 (for parameter b), respectively. These values were reduced to 0.69 and 0.21 (for parameter a) and to 1.68 and 0.38 (for parameter b) when the results were averaged for each site and when the sites with residual or cemented soils were excluded. The resulting mean normalized load-settlement curve ($a = 0.69$ and $b = 1.68$) and the 125 best-fit hyperbolic load-settlement curves are presented on Figure 1. The curves indicate that the load-settlement exhibited significant scatter about the mean relationship.

In a later study, Uzielli and Mayne (2012) assembled a database comprised of 30 footings that were subjected to axial loading. The database included 18 squares, 7 rectangular, and 5 circular

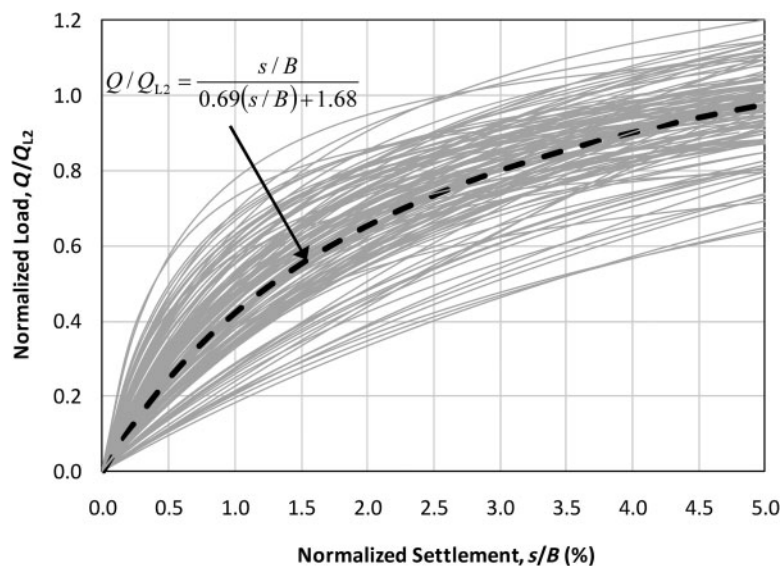


Figure 1. Best-fit and average hyperbolic normalized load-settlement curves for 125 load tests reported in Akbas and Kulhawy (2009a).

shallow foundations, with the equivalent footing width B varying from 0.5 to 6 m. The measured load-settlement curves for the different tests were normalized by dividing the settlement (s) by the footing width (B) and the applied stress (q_{app}) by the in situ net cone tip resistance $q_{c,net}$. Linear, hyperbolic, and power relationships were investigated to model the observed normalized load-settlement relationship of the 30 footings. The results of a comparative assessment of the performance of the three models indicated that the power model performed better than the other two models.

Despite the fact that the derived normalized hyperbolic load-settlement curve shown on Figure 1 constitutes the first rigorous attempt for modeling the full load-settlement behavior of footings on granular soils, a closer look at the actual data indicates that only 22 out of 167 test cases involve footings that have widths that are greater than 1.0 m, and only 14 footings with equivalent widths greater than 1.0 m were used to derive the load-settlement relationship on Figure 1. There is a need for validating and updating this relationship with test cases involving footings of practical field scale. There is a wealth of data in the literature on point measurements of settlement and load for such footings. Point measurements are the result of load tests whereby one settlement reading is obtained for a given applied load, restricting the results to a single point rather than a full load-settlement relationship.

The paper aims at using point measurements of settlement and load from full-scale footings to (1) update the current normalized load-settlement relationship which is mainly derived from footings with widths that are smaller than 1.0 m, (2) evaluate the uncertainty in the predictions of the updated load-settlement relationship, and (3) quantify the effect of the updating process on the SLS design of shallow foundations using illustrative examples. The updating process will be conducted by utilizing the First-Order Second-Moment Bayesian approach (FSBM) presented in Gilbert (1999).

2. Load-settlement behavior of footings using point measurements

Akbas (2007) compiled a database of 426 cases involving point measurements of settlements and loads for shallow foundations on granular soils. The test cases included foundations ranging in equivalent widths from 0.25 m (plates) to 135 m (rafts). Since the database included 116 test cases that were extracted from the database of complete load-settlement curves (Akbas and Kulhawy 2009a), these test cases were excluded from the analysis, resulting in a

net number of original tests of 310. These point measurements of settlement and load were not used in the calibration of the model proposed by Akbas and Kulhawy (2009a). Thirty-five tests involved footings with widths that are less than 1 m, 204 tests involved footings with widths between 1 and 10 m, and 51 tests involved footings with widths greater than 10 m.

To utilize the database collected by Akbas (2007) in the assessment/updating of the normalized load-settlement relationship proposed in Figure 1, the point measurements had to be normalized with respect to B and Q_{L2} . This posed a problem since the value of Q_{L2} was not available for the point measurements. However, Akbas and Kulhawy (2009b) proposed a relationship between Q_{L2} and the conventional ultimate bearing capacity (Q_{tcp}) of the foundation. This relationship suggests that Q_{L2} could be estimated as a function of Q_{tcp} such that:

$$Q_{L2} = Q_{tcp} = Q_{tcp}^v + Q_{tcp}^q \text{ for footings with } B \text{ greater than 1.0 m} \quad (2)$$

$$Q_{L2} = Q_{tcp} = (Q_{tcp}^v/B) + Q_{tcp}^q \text{ for footings with } B \text{ less than or equal to 1.0 m} \quad (3)$$

An expression for Q_{tcp} , as defined by Akbas and Kulhawy (2009b), is presented in Appendix 1. Equations 2 and 3 could be used to evaluate Q_{L2} for each of the 310 tests mentioned above.

Since the accurate estimation of Q_{tcp} involves knowledge about soil properties that were not presented in Akbas (2007) for each case in the database, the ratio of Q/Q_{L2} was back-calculated from tabulated settlement predictions obtained and presented in Akbas (2007) using the model proposed in Figure 1. For example, assume that the measured normalized settlements (s/B) for one of the cases in Akbas (2007) is equal to 0.5% and that the normalized settlement that is predicted in Akbas (2007) for this case using the normalized load-settlement model by Akbas and Kulhawy (2009a) is 0.7%. Given the model parameters as $a = 0.69$ and $b = 1.68$, the value of Q/Q_{L2} for this case could be back-calculated from Equation 1 as $Q/Q_{L2} = 0.7 / (0.69 \times 0.7 + 1.68) = 0.32$. This back-calculated ratio of Q/Q_{L2} coupled with the ratio of the measured settlement to the footing width ($s/B = 0.5\%$ for this case) constitutes one point (among 310 points) to be used in the evaluation/updating process of the hyperbolic model presented in Figure 1.

The 310 normalized datapoints are plotted in Figure 2 together with the original mean load-settlement relationship proposed by Akbas and

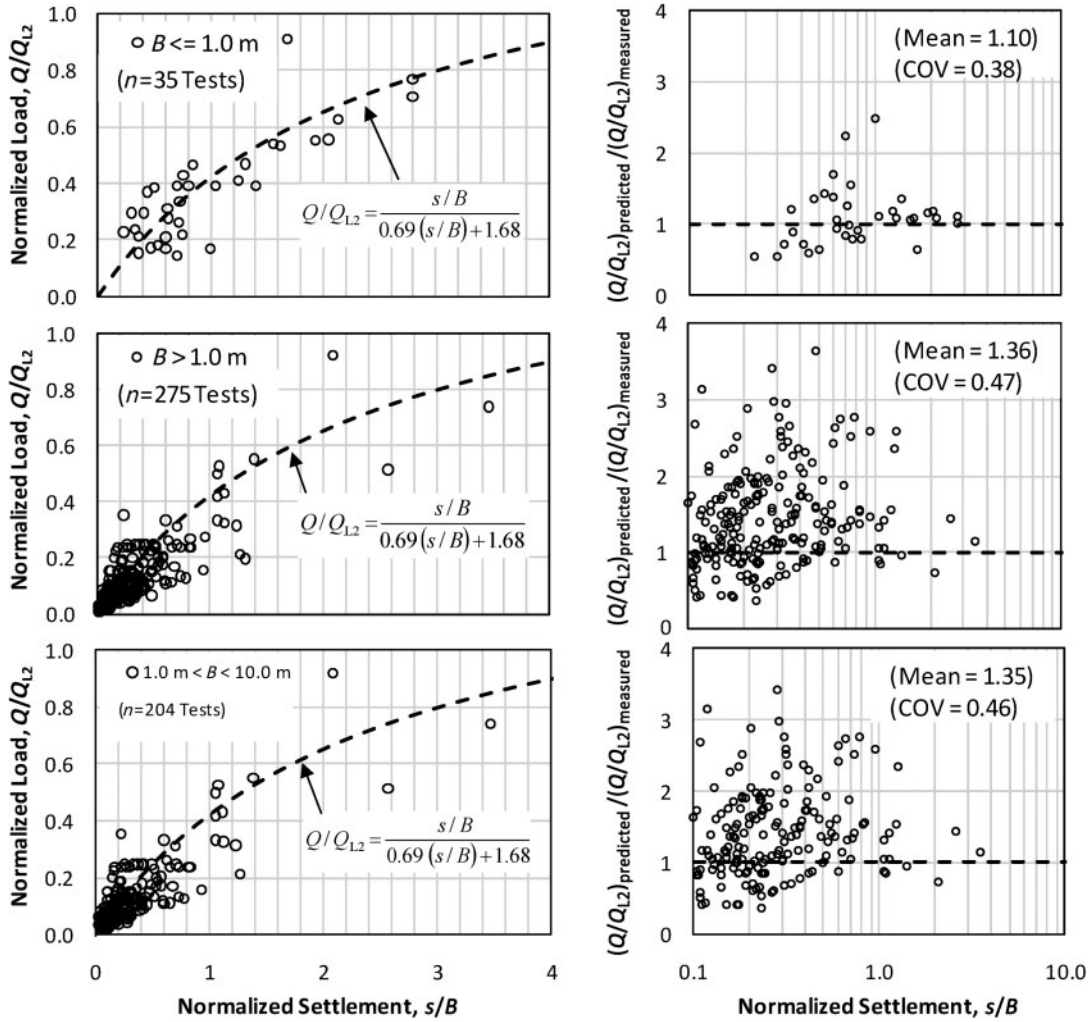


Figure 2. Normalized point measurements of load and settlement for different footing widths (Data from Akbas 2007).

Kulhawy (2009a). In Figure 2a, all the cases with a footing width B less than or equal to 1.0 m are included, while in Figure 2b, all the cases with a B that is greater than 1.0 m are included. The data presented in Figure 2a indicates that the hyperbolic model seems to provide an acceptable prediction of the point measurements with a B that is less than or equal to 1.0 m. An analysis of the data (35 test cases only) indicates that the ratio of predicted to measured Q/Q_{L2} for these small footings/plates was found to have a relatively unbiased mean value of only 1.10 and a reduced coefficient of variation (COV) of 0.38. On the other hand, an analysis of the ratio of predicted to measured Q/Q_{L2} for the tests with a footing width greater than 1.0 m (Figure 2b) indicates that on average, the hyperbolic model tends to overestimate the normalized load for a given normalized settlement. For these cases which involve footings of a practical field scale (275 test cases), the

mean value of the ratio of predicted to measured Q/Q_{L2} is equal to 1.36 with an associated coefficient of variation of 0.47.

The more effective predictive performance of the normalized hyperbolic model as exhibited in Figure 2a for footings with widths less than 1.0 m is related to the fact that the hyperbolic model (Akbas and Kulhawy 2009a) was derived from footings with widths that are generally smaller than 1.0 m (145 footings with $B < 1.0$ m from a total of 167 footings). This explains the reason for the bias in the predictions of the model increase from 1.1 to 1.36 for footings that are larger than 1.0 m. This finding is important, because it points to the importance of differentiating between foundations with widths less than 1.0 m from larger foundations (from a serviceability perspective). Such a differentiation between footings with widths that are less than 1.0 m and those that are greater than 1.0 m was adopted by

Akbas and Kulhawy (2009b) for shallow foundations on cohesionless soils from a bearing capacity perspective. Akbas and Kulhawy (2009b) separated footings with widths that are less than 1.0 m from footings with widths that are greater than 1.0 m when proposing an equation for calculating the bearing capacity of the foundation (see Equations 2 and 3).

The above discussion indicates that the hyperbolic model could be updated using data from full-scale footings ($B > 1.0$ m) to make it more applicable to footings of practical field scale. To test whether very large footings (basically rafts) might have biased the results, an additional analysis (Figure 2c) was conducted for foundations with widths that are confined to the range of 1–10 m. The normalized point measurements for such footings (204 test cases) were plotted on Figure 2c. The statistics of the ratio of predicted to measured Q/Q_{L2} for these footings were found to be similar to the case with $B > 1$ m, indicating a more-or-less negligible effect of very large footings (rafts) on the reported findings.

It is worth noting that although the mean ratio of predicted to measured Q/Q_{L2} for the hyperbolic model is in the order of 1.36 (for $B > 1.0$ m), this ratio increases if only the cases with s/B between 0.4 and 2.0% are included in the analysis. This range represents settlements that are expected for full-scale footings with widths ranging from 2.0 to 7.0 m and allowable settlements that are in the range of 2.5–5.0 cm. If only such cases are taken into consideration, the mean ratio of the predicted to measured Q/Q_{L2} increases to values of 1.56 and 1.58 for the cases involving footings with B greater than 1.0 m and B between 1.0 and 10.0 m, respectively. These results further reinforce the need for updating the curve proposed in Figure 1 using data for footings with widths that are greater than 1.0 m.

3. Probabilistic hyperbolic load-settlement model

3.1. General formulation

The hyperbolic model in Equation 1 could be represented probabilistically by considering that the normalized force Q/Q_{L2} for a given normalized displacement s/B is a random variable with a mean and a standard deviation that are represented by:

$$\mu_{Q/Q_{L2}} = \frac{s/B}{\Phi_1(s/B) + \Phi_2} \text{ and } \sigma_{Q/Q_{L2}} = e^{\Phi_3} \quad (4)$$

where Φ_1 , Φ_2 are the parameters of the mean hyperbolic model and e^{Φ_3} reflects the standard deviation in the value of Q/Q_{L2} about the predicted mean. The exponential term is used to ensure that

the standard deviation is a positive quantity. In the probabilistic model, the parameters (Φ_1 , Φ_2 , and Φ_3) were assumed to be random numbers that are defined by their means, variances, and covariances.

3.2. Prior statistics for model parameters

The prior estimates of the means of Φ_1 and Φ_2 were adopted from the statistics proposed by Akbas and Kulhawy (2009a) ($\mu_{\Phi_1} = 0.69$, $\mu_{\Phi_2} = 1.68$). The estimation of the prior variances of Φ_1 and Φ_2 on the other hand was not straightforward, since the coefficients of variation for Φ_1 and Φ_2 as presented in Akbas and Kulhawy (2009a) represent the variability in the individual load-settlement relationships for the different case studies, while the prior variances of Φ_1 and Φ_2 to be used in association with the probabilistic model in Equation (4) represent the uncertainty in the average load-settlement relationship. To get representative estimates of the prior variances of Φ_1 and Φ_2 , the variances reported in Akbas and Kulhawy (2009a) were reduced by dividing the variances by the number of cases n , to reflect the fact that the prior variances of Φ_1 and Φ_2 are associated with uncertainty in the average normalized load ($\mu^{Q/Q_{L2}}$) and not in the actual normalized load (Q/Q_{L2}). The division by the number of cases n assumes that these cases are statistically independent, which is a realistic assumption for the case at hand. The prior coefficients of variation of Φ_1 and Φ_2 were thus evaluated as $\text{COV}_{\Phi_1} = 0.21/\sqrt{25} = 0.042$ and $\text{COV}_{\Phi_2} = 0.38/\sqrt{25} = 0.075$. It should be noted that the number of cases n was taken as 25, to be consistent with the statistics presented in Akbas and Kulhawy (2009a) ($\mu_{\Phi_1} = 0.69$, $\text{COV}_{\Phi_1} = 0.21$, $\mu_{\Phi_2} = 1.68$, and $\text{COV}_{\Phi_2} = 0.38$) for the case where the results were averaged for each site and when the sites with residual or cemented soils were excluded.

An analysis of the 125 pairs of Φ_1 and Φ_2 indicated that the two parameters are negatively correlated with a correlation coefficient ρ of -0.69 . This estimate was used as a prior estimate of the correlation coefficient between Φ_1 and Φ_2 .

The parameter Φ_3 in Equation 4 defines the uncertainty in the load-settlement relationship, as reflected in $\sigma_{Q/Q_{L2}}$. The formulation of the probabilistic model is based on the assumption that $\sigma_{Q/Q_{L2}}$ is a constant that is independent of the s/B ratio. The validity of this assumption is verified on Figure 3a which shows the variation of $\sigma_{Q/Q_{L2}}$ with s/B for the 125 test cases reported in Akbas and Kulhawy (2009a). To compile this plot, the actual datapoints (about 1500 points) that form the 125 load-settlement curves (presented in Akbas 2007) were digitized and

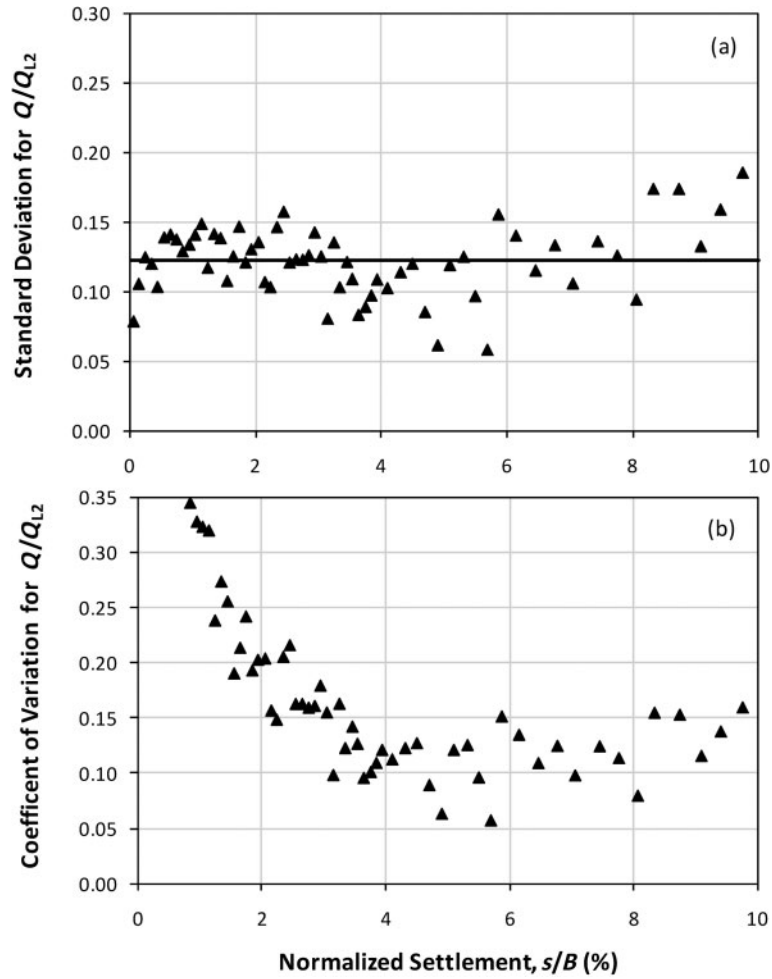


Figure 3. Variation of the standard deviation and the coefficient of variation of Q/Q_{L2} with normalized settlement s/B .

an effort was made to compute the standard deviation of Q/Q_{L2} about the mean load-settlement relationship for representative intervals of s/B . A similar effort was made to compute the variation of the $cov_{Q/Q_{L2}}$ with s/B for comparison. The variation of $\sigma_{Q/Q_{L2}}$ and $cov_{Q/Q_{L2}}$ with s/B is shown on Figures 3a, and 3b, respectively. Results indicate that $\sigma_{Q/Q_{L2}}$ could be considered to be independent of s/B , while the $cov_{Q/Q_{L2}}$ is strongly dependent on s/B , especially at s/B ratios that are less than 4.0% which are relevant to serviceability problems.

In order not to complicate the probabilistic load-settlement model, a decision was made to assume that $\sigma_{Q/Q_{L2}}$ in Equation 4 could be considered as a constant, with a mean of 0.122 and a standard deviation of 0.025. Since the actual model parameter that defines $\sigma_{Q/Q_{L2}}$ is Φ_3 , the prior mean and coefficient of variation of Φ_3 were evaluated from the mean and standard deviation of $\sigma_{Q/Q_{L2}}$ as $\mu_{\Phi_3} = -2.1$ and $COV_{\Phi_3} = 0.2$. Since there is no physical

reason for Φ_3 to be correlated to either Φ_1 or Φ_2 , it was assumed that Φ_3 was statistically independent from Φ_1 and Φ_2 .

The prior distribution of the model parameters will be assumed to be a multivariate normal distribution that is characterized by a mean vector $\mu_{\bar{\Phi}}$ and a covariance matrix $C_{\bar{\Phi}}$ such that:

$$\mu_{\bar{\Phi}} = \begin{bmatrix} 0.69 \\ 1.68 \\ -2.1 \end{bmatrix} \text{ and} \quad (5)$$

$$C_{\bar{\Phi}} = \begin{bmatrix} (0.029)^2 & -0.0025 & 0 \\ -0.0025 & (0.126)^2 & 0 \\ 0 & 0 & (0.420)^2 \end{bmatrix}$$

4. First-order second moment Bayesian approach (FSBM)

The FSBM proposed by Gilbert (1999) was used to calibrate the probabilistic hyperbolic model using normalized point measurements of settlement and

load derived from full-scale footings. Following the derivation in Gilbert (1999), the FSBM uses Bayes' theorem (Equation 6) to update the probability distribution of the model parameters for a given set of data.

$$f_{\vec{\Phi}|\vec{\varepsilon}}(\vec{\Phi}|\vec{\varepsilon}) = L(\vec{\varepsilon}|\vec{\Phi})f_{\vec{\Phi}}(\vec{\Phi}) / \int_{-\infty}^{+\infty} \dots \int_{-\infty}^{+\infty} L(\vec{\varepsilon}|\vec{\Phi})f_{\vec{\Phi}}(\vec{\Phi})d\Phi_1 \dots d\Phi_n \quad (6)$$

where $f_{\vec{\Phi}|\vec{\varepsilon}}(\vec{\Phi}|\vec{\varepsilon})$ and $f_{\vec{\Phi}}(\vec{\Phi})$ are the updated (given the new data $\vec{\varepsilon}$) and prior joint distributions of the model parameters $\vec{\Phi}$, $L(\vec{\varepsilon}|\vec{\Phi})$ is the likelihood function, and $\int_{-\infty}^{+\infty} \dots \int_{-\infty}^{+\infty} L(\vec{\varepsilon}|\vec{\Phi})f_{\vec{\Phi}}(\vec{\Phi})d\Phi_1 \dots d\Phi_n$ is a normalizing constant. The first (updated mean vector $\vec{\mu}_{\vec{\Phi}|\vec{\varepsilon}}$) and second (updated covariance matrix $C_{\vec{\Phi}|\vec{\varepsilon}}$) moments of the calibrated model parameters are derived from a second-order approximation of Equation 6 by approximating the natural logarithm of the likelihood function with a second-order Taylor series. The expansion point $\vec{\Phi}^*$ which maximizes $g(\vec{\Phi})$ (the natural logarithm of the likelihood function, see Appendix 2) is then obtained and used to calculate approximations for the updated mean vector $\vec{\mu}_{\vec{\Phi}|\vec{\varepsilon}}$ and the updated covariance matrix $C_{\vec{\Phi}|\vec{\varepsilon}}$ (Gilbert 1999):

$$\vec{\mu}_{\vec{\Phi}|\vec{\varepsilon}} = C_{\vec{\Phi}|\vec{\varepsilon}} \left\{ \left[\frac{-\delta^2 g}{\delta\Phi_i \delta\Phi_j} \right]_{\vec{\Phi}^*} \vec{\Phi}^* + C_{\vec{\Phi}}^{-1} \vec{\mu}_{\vec{\Phi}} \right\} \quad (7)$$

$$C_{\vec{\Phi}|\vec{\varepsilon}} = \left[\left[\frac{-\delta^2 g}{\delta\Phi_i \delta\Phi_j} \right]_{\vec{\Phi}^*} + C_{\vec{\Phi}}^{-1} \right]^{-1} \quad (8)$$

It should be noted that the updated moments that result from the FSBM method are approximate values. These updated moments are based on prior information and the information contained in the likelihood function. The above formulation assumes that the prior model parameters follow a multivariate normal distribution, and as a result, the approximate distribution for the updated model parameters is also a multivariate normal distribution. The updated mean value obtained using the FSBM is a weighted average of the prior mean value and maximum likelihood point for the data-set (Gilbert 1999). Therefore, if more information about a given parameter is provided in the data-set (ex. larger data-set of observed measurements), the more this information will be weighted compared to the prior information. The updated covariance matrix calculated by the FSBM provides the updated variance of each parameter and the covariance between each

parameter. In addition, correlation coefficients can be calculated between each model parameter to identify related pairs of parameters.

The FSBM was developed to provide a practical Bayesian method for problems with multiple model parameters, large data-sets, and various data distributions. As with any First-Order Second-Moment method, the results of the FSBM are considered approximate, especially for cases involving nonlinear models and large uncertainties in model parameters. To provide an indication of the advantages and limitations of the FSBM, Gilbert (1999) presented an example involving a model of pile capacity at an offshore site. The probabilistic model involved 7 parameters and included a spatial variability model that caters for spatial correlation in pile capacity. Gilbert (1999) checked the validity of the approximate results obtained from the FSBM using Monte Carlo simulations and concluded that the results of the FSBM compared favorably to the Monte Carlo simulation results. It was also concluded that the FSBM approximations are better for the model parameters describing the mean and standard deviation of the pile capacity than for parameters describing the correlation structure. The main advantage of the FSBM is that the results were obtained in less than 1/10000 of the computational time required for the Monte Carlo analysis leading to the conclusion that FSBM provides a far more practical means of analyzing data than Monte Carlo simulations.

5. Updated probabilistic hyperbolic load-settlement model

The updating process of the hyperbolic relationship was conducted using two sets of data. The first set involves the 310 cases representing Q/Q_{L2} and s/B point measurements of all the foundations in the Akbas (2007) database (Cases I, II, and III), while the second set (Cases IV, V, and VI) was restricted to the 204 load cases with footing widths that range from 1.0 to 10.0 m. For both sets, three cases were analyzed to investigate the effect of correlation between multiple datapoints in a given site on the results of the updating process.

It is worth noting that since the estimation of Q_{L2} requires the utilization of the bearing capacity model that is proposed by Akbas and Kulhawy (2009b) and presented in Equations 2 and 3 (and Appendix 1), the estimate of Q_{L2} will have a degree of uncertainty associated with it. To limit the scope of this paper and its length, assessing the value of this uncertainty and incorporating it in the updating process was

judged to be not feasible. This could be a subject of future work.

5.1. Bayesian updating assuming statistically independent within-site data

The analysis was first conducted for the case where all the observed datapoints were assumed to be statistically independent (correlation coefficient $\rho = 0$) even if the datapoints came from multiple footing tests in the same site. This assumption may not be practical, given that results from a given site are expected to be positively correlated. If the positive correlation is neglected, sites with multiple datapoints could bias the resulting updated load-settlement relationship. The presence or lack of correlation affects the updating process through (1) the resulting expansion point $\vec{\Phi}^*$ which maximizes $g(\vec{\Phi})$ (the natural logarithm of the likelihood function), and (2) the second derivatives of the natural logarithm of the likelihood $\frac{\partial^2 g}{\partial \Phi_i \partial \Phi_j}$ which affect the updated means and covariance matrix of the model parameters in Equations 7 and 8.

The prior means, coefficients of variation, and correlation coefficients of the model parameters are presented in Table 1. Assuming statistically independent observed datapoints, the Bayesian updating process was conducted using the 310 cases representing all the foundations (Case I) and using the 204 load cases with footing widths that range from 1.0 to 10.0 m (Case IV). The resulting updated model parameters are included in Table 1 for comparison.

Results in Table 1 indicate that the resulting updated mean values of Φ_1 and Φ_2 are 0.64 and 2.08, respectively (compared to 0.69 and 1.68 for the prior case), and are insensitive to the number of cases in the two data-sets. Since the parameters Φ_1 and Φ_2 define the mean hyperbolic load-settlement relationship, the difference between the prior and updated relationships could be illustrated graphically (see Figure 4). As expected, the updated load-settlement curve is lower than the original curve proposed by Akbas and Kulhawy (2009a). For the practical range of normalized settlements ($0.5\% < s/B < 2.0\%$), the updated curve provides a better fit to the measured data. For larger settlements ($s/B > 2\%$), the lack of data makes the assessment of the behavior inconclusive. As such, there is a need for gathering more information of load and settlement in this high settlement range for practical footings on granular soil.

The parameters that affect uncertainty in the load-settlement relationships are the coefficients of variation in Φ_1 and Φ_2 in addition to the mean and coefficient of variation of Φ_3 , which could be combined using a first-order approximation (Gilbert 1999) to produce an estimate of the overall uncertainty. Results in Table 1 indicate that the updated coefficients of variation for Φ_1 and Φ_2 were slightly reduced ($0.038 < \text{COV}_{\Phi_1} < 0.039$ and $0.03 < \text{COV}_{\Phi_2} < 0.036$), compared to their prior estimates. However, what governs the uncertainty in the load-settlement relationship is the parameter Φ_3 which determines the standard deviation of Q/Q_{L2} for a given s/B . Results in Table 1 for cases I (310 test

Table 1. Results of the Bayesian updating process for different prior scenarios.

Model parameters	Updating using all data (310 tests)			Updating using footings with $1.0 \text{ m} < B < 10.0 \text{ m}$ (204 tests)			
	Case I	Case II	Case III	Case IV	Case V	Case VI	
	($\rho = 0$, same site)	($\rho = 0.2$, same site)	($\rho = 0.4$, same site)	($\rho = 0$, same site)	($\rho = 0.2$, same site)	($\rho = 0.4$, same site)	
	Prior	Updated	Updated	Updated	Updated	Updated	Updated
μ_{Φ_1}	0.69	0.64	0.64	0.64	0.64	0.64	0.64
COV_{Φ_1}	0.042	0.038	0.039	0.040	0.039	0.040	0.041
μ_{Φ_2}	1.68	2.07	2.09	2.10	2.08	2.09	2.10
COV_{Φ_2}	0.075	0.030	0.035	0.038	0.036	0.041	0.044
μ_{Φ_3}	-2.1	-2.66	-2.68	-2.63	-2.70	-2.77	-2.75
COV_{Φ_3}	0.20	0.015	0.015	0.015	0.018	0.018	0.018
ρ_{Φ_1, Φ_2}	-0.69	-0.62	-0.64	-0.64	-0.60	-0.64	-0.65
ρ_{Φ_1, Φ_3}	0	0	0	0	0	0	0
ρ_{Φ_2, Φ_3}	0	0	0	0	0	0	0

cases) and IV (204 test cases) assuming statistical independency between datapoints in a given site indicate a significant reduction in the standard deviation of Q/Q_{L2} for a given s/B . This is reflected in the reduced updated mean value of Φ_3 (-2.66 to -2.7), compared to its prior mean (-2.1). These reductions translate into a reduction from 0.122 to about 0.068 in the standard deviation of Q/Q_{L2} for a given s/B . Moreover, the uncertainty in the parameter Φ_3 was also reduced dramatically in the updating process, reflecting a high degree of confidence in the standard deviation of the updated load-settlement model.

The parameters that affect uncertainty in the load-settlement relationships were combined using a first-order approximation (Gilbert 1999) to produce an estimate of the overall uncertainty in the updated load-settlement relationship. Details regarding how the uncertainties were combined are presented in Appendix 3. The resulting uncertainty is reflected in Figure 4 in the form of curves representing plus and minus one and two standard deviations about the mean relationship. These curves represent uncertainty in Q/Q_{L2} for the case where test cases in a given site were assumed to be statistically independent in the updating process.

5.2. Bayesian updating assuming correlation between within-site data

Results from load tests that are conducted within the same site are expected to be correlated. The degree of correlation could be affected by many parameters including the distance between the locations of the

different tests, the lateral and vertical variabilities of the soil within the site, variability in the sizes of footings, and variability in the magnitude of the test loads.

An attempt to quantify the degree of correlation between datapoints within a given site was conducted for the available data. All sites with more than 5 load tests were included in the analysis which consisted of an effort to quantify the autocorrelation coefficient between within-site test points. Only 12 sites included more than 5 datapoints, as indicated in Figure 5, which shows the point measurements in relation to the prior mean load-settlement relationship proposed by Akbas and Kulhawy (2009a). The statistical analysis was based on a quantification of the degree of correlation between the residuals (u_i) of the datapoints which were calculated by subtracting the measured Q/Q_{L2} at a given s/B by the predicted mean Q/Q_{L2} value at the same s/B ratio. The sample correlation coefficient for the within-site data was then evaluated using Equation 8 as the ratio of the covariance of Q/Q_{L2} measurements in a given site to the variance of all the residuals in the data-set such that:

$$\rho = \frac{E(u_i u_j)}{\sigma_{(u)}^2} \tag{9}$$

where ρ is the sample correlation coefficient for measurements in a given site, u_i and u_j are pairs of residuals of Q/Q_{L2} measurements in a given site, $E(u_i u_j)$ is the expected value of the product of the pairs of residuals of Q/Q_{L2} measurements in a given site (covariance between pairs of Q/Q_{L2} measurements

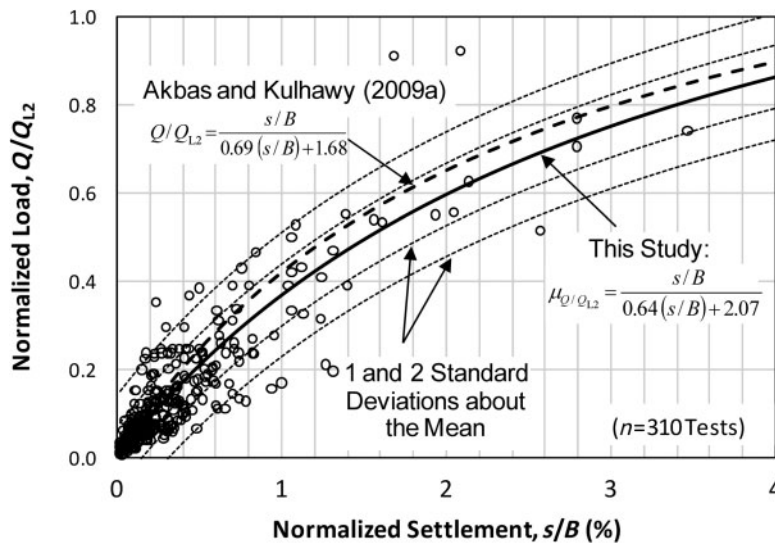


Figure 4. Prior normalized load-settlement relationship and updated mean and plus and minus 1 and 2 standard deviations about the mean load-settlement relationships for no within-site test correlation, ($\rho = 0$).

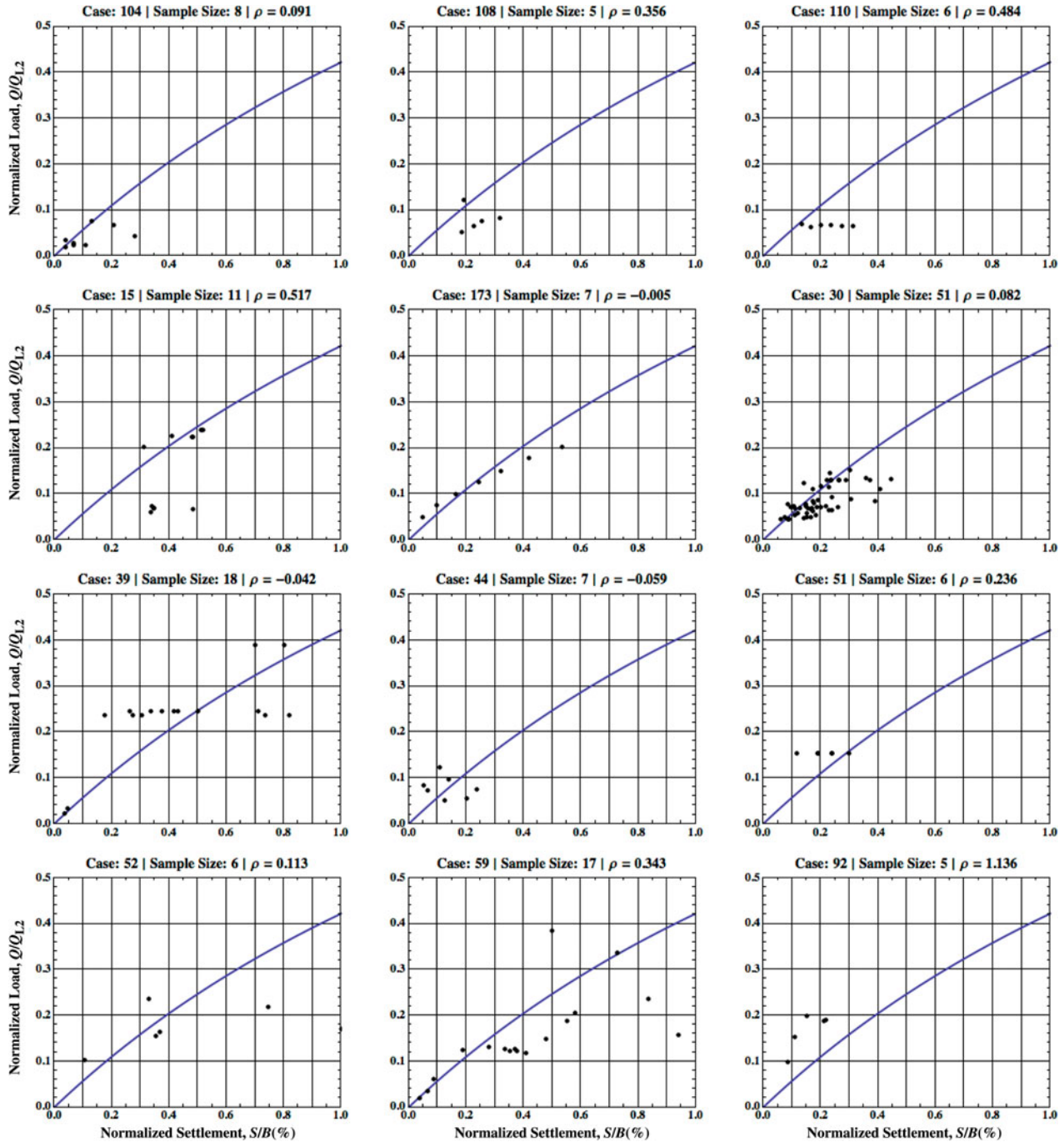


Figure 5. Assessment of the degree of correlation in load-settlement measurements within a given site.

in a given site), and $\sigma_{(u)}^2$ is the variance of all the residuals of Q/Q_{L2} in the data-set.

The resulting sample correlation coefficients are summarized on Figure 5 for all the sites with more than 5 cases. Results indicate that the correlation coefficient could range from -0.06 (indicating very weak correlation) to about 1 (indicating perfect correlation), but the majority of cases involved positive correlation coefficients ranging from about

0.1 to 0.5 (8 out of 12 cases). The average correlation coefficient was found to be 0.26.

To investigate the effect of correlation between within-site data on the results of the updating process, the Bayesian updating exercise was repeated assuming representative positive correlation coefficients $\rho = 0.2$ (cases II and V in Table 1) and 0.4 (cases III, and VI in Table 1), respectively. As expected, the inclusion of a non-zero correlation

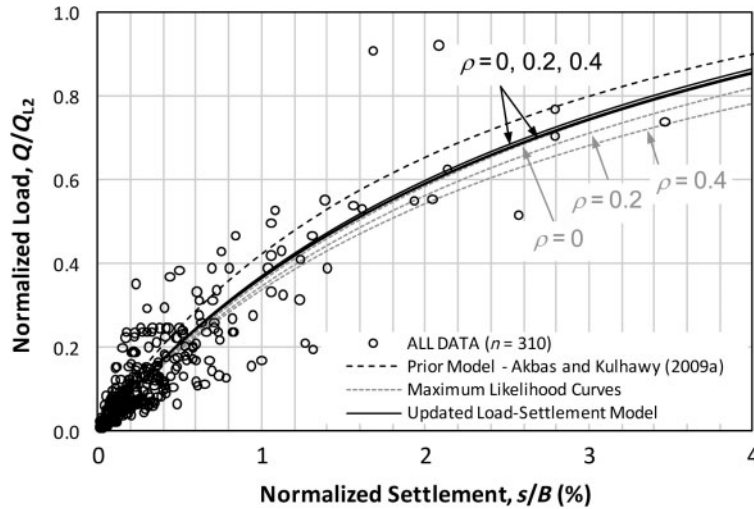


Figure 6. Effect of correlation between within-site measurements on the maximum likelihood and updated load-settlement relationships.

coefficient was found to have a notable effect on the expansion point $\vec{\Phi}^*$ which maximizes $g(\vec{\Phi})$ (the natural logarithm of the likelihood function). To illustrate the effect of assuming different correlation coefficients on the updating process, the resulting $\vec{\Phi}^*$'s (particularly Φ_1^* and Φ_2^*) were used to calculate and plot the normalized load-settlement curves that represent curves of maximum likelihood for different assumptions of the correlation for data within the same site. These curves are shown as gray dotted lines in Figure 6. Also shown on Figure 6 are the prior (Akbas and Kulhawy 2009a) and updated (for different correlation coefficients) normalized load-settlement relationships.

The results on Figure 6 indicate that the assumption of different correlation coefficients resulted in different maximum likelihood curves. However, the effect of assuming different correlation coefficients on the updated load-settlement relationships was found to be insignificant, as indicated in the figure. This could be explained by the fact that the results of the updating process are also affected by the statistics of the prior model parameters which for this example had a significant weight in the Bayesian analysis, thus obscuring the effect of correlation on the results of the updated model parameters.

Based on the above results, it could be concluded that the assumption of correlation between point measurements in a given site did not affect the results of the updating process. Moreover, the results in Table 1 also indicated that the updating process with all the data (310 points) resulted in very similar updated model parameters compared to the case with the footings with $1 \text{ m} < B < 10.0 \text{ m}$ (204 cases). As a result, it could be assumed that the updated load-settlement relationship

presented in Figure 4 for the case involving all the datapoints assuming no correlation for within-site data (Case I in Table 1) is representative of all the other cases analyzed in this study. As a result, this updated load-settlement relationship will be used in this paper to illustrate the use of the updated relationship in solving serviceability limit state (SLS) problems for footings on granular soils.

6. Illustrative example

An example that illustrates the use of the updated normalized load-settlement relationship in solving serviceability limit state (SLS) design problems for footings on granular soils is presented in this section. The example involves square footings with widths of 1.5, 2.5, and 3.0 m that are embedded 0.8 m in a medium dense sand layer with a friction angle of 36° and a modulus of elasticity of 40,000 kPa. Since the objective of the example is to portray the effect of the load-settlement model on the SLS capacity of the footings, the effect of uncertainty in soil properties due to spatial variability on the settlement will be ignored in the analysis. In addition, a practical design scenario whereby an allowable or tolerable settlement is used as a design criterion will be adopted in lieu of more rigorous but less practical approaches that are based on tolerable angular distortions between footings. In such approaches, the effect of the settlement prediction model is generally masked by the governing effect of spatial variability in soil properties between adjacent footings. Akbas and Kulhawy (2009b) present a rigorous and robust approach for calibrating resistance/deformation factors to account for angular distortions between adjacent footings. In the example

presented in this section, tolerable or allowable settlements, discussed below, will be used as the basis for the SLS design as is the case in practical design problems involving footings on granular soils.

The limiting tolerable or allowable foundation settlement (referred to in this paper as δ_{all}) was examined by many researchers (e.g., Skempton and MacDonald 1956; Zhang and Ng 2005). Skempton and MacDonald (1956) report that the maximum settlement of a foundation on sand (in inches) is generally equal to about 600 times the angular distortion of the foundation. They also report that damage for typical buildings is observed at an angular distortion of about 1/300, indicating that the maximum settlement that can be tolerated by an isolated foundation on sand is about 2 inches or 5 cm. By applying a factor of safety of 1.5 to the allowable angular distortion, they recommend that the tolerable maximum settlement should be taken as 1.5 inches or 3.75 cm. Using a database of over 300 buildings, Zhang and Ng (2005) reported that the maximum allowable or tolerable settlement δ_{all} varies over a wide range and follows a lognormal distribution that has a mean of 12.9 cms and a coefficient of variation of 0.558. However, they do not report statistics that distinguish between shallow foundations on sand and clay. Wang and Kulhawy (2008) report that these statistics are significantly larger than the allowable settlement limit of 2.5 cms that is used frequently in deterministic design. Zhang and Ng (2005) state that the small allowable settlement (2.5 cm) is obtained by dividing the large limiting tolerable settlements that are observed in databases by appropriate safety factors or by adopting the lower-bound of the observed tolerable settlement.

For the exercise presented in this paper, a typical deterministic δ_{all} of 2.5 cm will be initially adopted to calculate a deterministic estimate of the SLS capacity (Q_{SLS}) of the 3 square foundations described earlier. The analysis will be conducted for the prior and updated normalized load-settlement relationships presented in Figure 4. In addition, the SLS capacity resulting from two commonly used SPT-based settlement prediction models (Meyerhof 1965; Burland and Burbidge 1985) will be computed for comparison with the more recent normalized-load settlement models. The Q_{SLS} that is computed from these traditional models is given by Equations 10 and 11, respectively, as:

$$Q_{\text{SLS}} = \frac{N_{60}(B + 0.3)^2}{2.12 \left(1 - \frac{D_f}{4B}\right) \lambda} \delta_{\text{all}} \text{ for } B > 1.22 \text{ m} \quad (10)$$

$$Q_{\text{SLS}} = \frac{B^{1.3}(N_{60})^{1.4}}{1.71 \lambda} \delta_{\text{all}} + \gamma D_f B^2 \quad (11)$$

where N_{60} is the uncorrected blow count from standard penetration tests (SPT), D_f is the embedment depth of the footing, γ is the unit weight of the overburden soil, B is the width of the square foundation, and λ is a random variable representing the model uncertainty (to be included only in reliability calculations and not in the deterministic calculations). For the SPT-based models, N_{60} was taken to be equal to 18 to reflect medium dense sand with a friction angle of about 36 degrees.

For the three footing widths of 1.5, 2.5, and 3.0 m, the computed SLS capacities for a deterministic allowable settlement of 2.5 cm are presented in Figure 7. In the computation of the SLS capacities for the prior and updated hyperbolic models, the parameter Q_{L2} was predicted using Equation 2 to be equal to Q_{tcp} which was in turn calculated using Equation A.1 presented in Appendix 1. Results in Figure 7 indicate that the updated mean normalized load-settlement relationship that is presented in Figure 4 resulted in a Q_{SLS} that is about 15% smaller than that predicted using the prior mean normalized relationship presented by Akbas and Kulhawy (2009a). As an illustration, Q_{SLS} decreased from 3068 kN (prior case) to 2683 kN (updated case) for the footing with a width of 2.5 m. For comparison, the Burland and Burbidge (1985) SPT-based method resulted in an intermediate Q_{SLS} of 2852 kN while the conservative SPT-based Meyerhof (1965) approach resulted in a reduced Q_{SLS} of 1809 kN.

The SLS design capacities that are presented in Figure 7 result from a deterministic analysis where the uncertainty in the load-settlement relationship and the uncertainty in the allowable or tolerable displacements are ignored. Conventional reliability-based design codes generally apply reliability principals to the ultimate limit state (ULS) design, and ignore these principals in serviceability limit state design (Wang and Kulhawy 2008). In this example, an attempt is made to evaluate the probability of excessive settlement for a foundation on granular soil based on a reliability approach that takes into consideration the serviceability limit state of the foundation. The probability of failure for the SLS design can be obtained from Equation 12 such that:

$$p_f = \text{Prob}(Q_{\text{SLS}} < P) \text{ and } \beta_{\text{SLS}} = -\Phi^{-1}(p_f) \quad (12)$$

where Q_{SLS} , as defined earlier, is the serviceability limit state capacity, P is the applied load, Φ^{-1} is the inverse of the standard normal probability distribution function, and β_{SLS} is SLS reliability index.

The SLS reliability analysis requires a quantification of the uncertainty in Q_{SLS} and in the applied

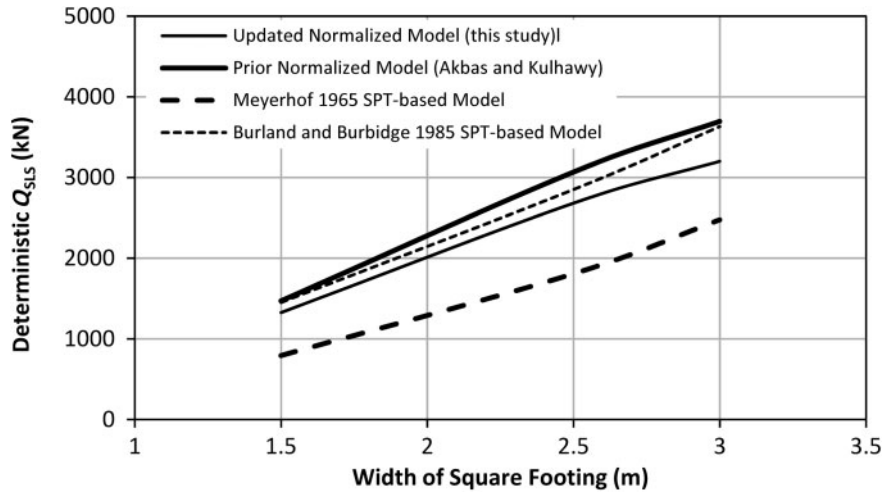


Figure 7. Effect of the load-settlement model on the SLS capacity of footings with different widths B (assuming a deterministic $\delta_{all} = 2.5$ cm).

load P . For the prior and updated normalized load-settlement relationships analyzed in this paper, the mean and standard deviation of Q_{SLS} for a given s/B ratio could be readily evaluated, given the probabilistic nature of the normalized load-settlement model. For the SPT-based methods of Meyerhof and Burland and Burbidge (1985), the parameter λ (Equations 10 and 11) which is a random variable representing the ratio of the “actual” settlement to the “predicted” settlement could be used for this purpose. Najjar and Sadek (2010) report means and COVs for λ of 0.65 and 0.76 for the Meyerhof (1965) model and 0.96 and 0.65 for the Burland and Burbidge (1985) model based on a database comprising 66 load test cases compiled by Berardi and Lancellotta (1991). These statistics could be used in Equations 10 and 11 to account for model uncertainty in the two SPT-based methods.

Since previous research shows that the tolerable or allowable settlement is also expected to be an uncertain parameter (Skempton and MacDonald 1956 and Zhang and Ng 2005), an effort was made to include the uncertainty in δ_{all} in the calculation of the uncertainty in Q_{SLS} . The mean of 12.9 cms and coefficient of variation of 0.558 reported by Zhang and Ng (2005) for the maximum allowable or tolerable settlement are based on cases of footings on sands and clays. To estimate the statistics of δ_{all} specifically for foundations on sand, data from 10 cases presented in Skempton and MacDonald (1956) were analyzed. The data indicate that the recommended δ_{all} of 5 cm (inferred by Skempton and MacDonald) is a representative mean value and that the scatter around that mean can be represented by a COV of about 0.2. In this study, δ_{all} will be assumed

to be a random variable having a mean of 5 cm and a COV of 0.2.

A first-order approximation was used to combine model uncertainty and uncertainty in the allowable or tolerable settlement to estimate the first two moments (mean and variance) of Q_{SLS} (see Appendix 3). Uncertainty due to spatial variability in soil properties was intentionally ignored from the analysis so as not to obscure the effect of the model uncertainty on the resulting SLS probabilities of failure. Such uncertainties could be included in any future study that is aimed at recommending safety factors or resistance/deformation factors in the SLS design of footings.

The calculated means and COVs for the SLS footing capacities are presented in Table 2. Results indicate that the mean of Q_{SLS} and the COV of Q_{SLS} are consistently larger in the SPT-based methods compared to the normalized load-settlement models. These larger mean values in the SPT-based models are largely due to the linear relationship that is inherent in these models between load and settlement. Since the mean Q_{SLS} corresponds to a relatively large mean tolerable settlement of 5 cm, the mean Q_{SLS} in the nonlinear normalized hyperbolic model was found to be much smaller than that calculated in the linear SPT-based models for the same displacement. The larger COVs in the SPT-based models could also be attributed to the linear relationship assumed in the models coupled with the relatively large model uncertainties that were originally inherent in these two models (COVs of 0.76 and 0.65). As an illustration, for the linear load-settlement relationship, predicted Q_{SLS} values corresponding to s/B values that are plus or minus two standard deviations about a given mean s/B value are expected

Table 2. Statistics of Q_{SLS} for different load-settlement models and footings widths (assume δ_{all} is uncertain with mean of 5 cm and a COV of 0.2).

Load-settlement model	$B = 1.5$ m		$B = 2.5$ m		$B = 3.0$ m	
	Mean Q_{SLS}	COV Q_{SLS}	Mean Q_{SLS}	COV Q_{SLS}	Mean Q_{SLS}	COV Q_{SLS}
Prior (s/B vs. Q/Q_{L2})	2100	0.20	4726	0.25	5900	0.28
Updated (s/B vs. Q/Q_{L2})	1975	0.13	4363	0.17	5300	0.19
Meyerhof (1965)	2442	0.79	5566	0.79	7621	0.79
Burland and Burbidge (1985)	2987	0.67	5833	0.67	7411	0.67

to exhibit a wider range than Q_{SLS} values that correspond to plus or minus two standard deviations about the same mean for a nonlinear hyperbolic relationship. This would lead to larger COVs for the linear relationships in comparison to the hyperbolic relationship.

To illustrate the difference in the resulting uncertainty in Q_{SLS} , the case of footings with $B = 2.5$ m was considered and plots showing typical lognormal probability density functions (PDF) that are described by the means and COVs presented in Table 2 are shown on Figure 8 for comparison. The PDFs clearly illustrate the reduced uncertainty which is exhibited in the Q_{SLS} distributions that are associated with the prior and updated normalized load-settlement relationships in comparison to the more traditional SPT-based methods. A comparison between the prior and updated PDFs of Q_{SLS} for the normalized load-settlement models indicates that the left-hand tail of the distribution which will govern the SLS probability of failure in any reliability analysis is slightly shifted to the left in the case of the prior distribution. It is thus expected that the reduced uncertainty that was exhibited in the updated distribution (COV = 0.17) compared to the prior distribution (COV = 0.25) will result in a higher reliability for the updated model.

To quantify the effect of the load-settlement model on the probability of a SLS failure (or reliability index) of the foundations, a reliability analysis was conducted using the Q_{SLS} distributions shown in Figure 8. The load distribution for each case was also taken as a lognormal distribution with a typical COV of 0.15. For comparison, the coefficients of variation specified by AASHTO (2004) to represent the uncertainty in bridge loads are 0.13 and 0.18 for the dead and live loads, respectively. The mean of the load distribution was assumed to be equal to a nominal load that corresponds to a deterministic settlement of 2.5 cm for each model, multiplied by a bias factor of 1.1 to account for a 10% difference (conservatism) between the mean and nominal load, as is the convention. The assumption that the nominal load is equal to the load that will result in a deterministic settlement of 2.5 cm is in line with current design practice where no factors of safety are assumed in the SLS design of foundations.

The calculated SLS reliability indices and associated probabilities of failure are presented in Figures 9a and 9b, respectively. As expected, results indicate that the updated normalized load-settlement relationship resulted in the lowest probability of failure ($p_f \sim 0.006$ and $\beta_{SLS} \sim 2.5$), while the SPT-based

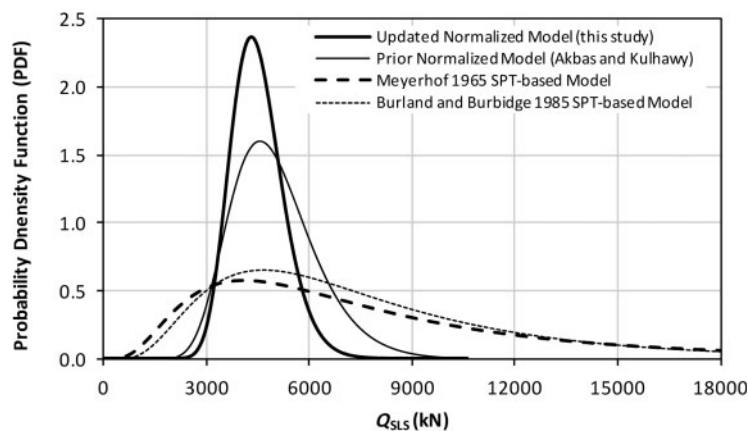


Figure 8. Probability density functions for Q_{SLS} ($B = 2.5$ m).

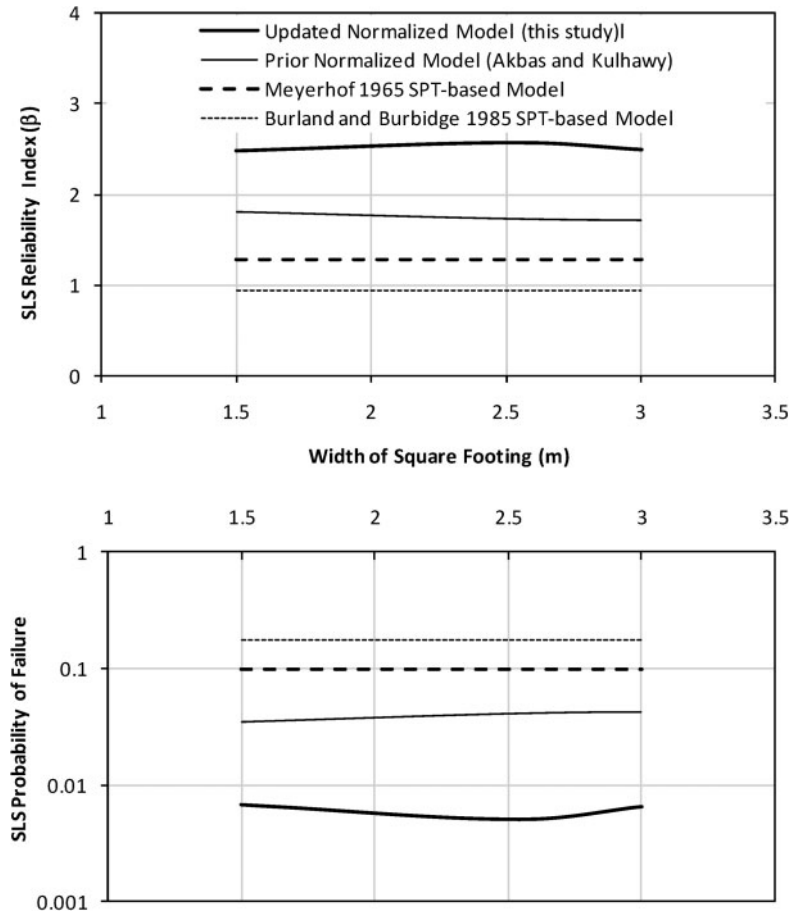


Figure 9. Variation of (a) the SLS reliability index and (b) the SLS probability of failure with footing widths (assume COV of load = 0.15).

methods resulted in the highest probability of failure ($p_f \sim 0.10$ to 0.17 and $\beta_{SLS} \sim 0.94$ to 1.28). The probabilities of failure associated with the prior normalized load-settlement model (Akbas and Kulhawy 2009a) were slightly larger ($p_f \sim 0.04$ and $\beta_{SLS} \sim 1.75$) than the updated normalized model due to the reduced uncertainty in the updated model. These results were found to be insensitive to the assumed width of the footing B . The significantly reduced reliability of the SPT-based models is largely due to their inherent linear relationship between load and settlement and their relatively large model uncertainties.

7. Conclusions and future work

Based on the results of a Bayesian process that targeted updating the normalized load-settlement relationship proposed by Akbas and Kulhawy (2009a), the following conclusions can be drawn based on the analyses conducted in this paper:

- (1) For a given settlement, the normalized hyperbolic load-settlement relationship proposed by Akbas and Kulhawy (2009a) was found to slightly overpredict the point measurements of load obtained from full-scale footings, with the mean value of the ratio of predicted to measured Q/Q_{L2} being in the range of 1.35–1.36. For normalized settlements that are more representative of practical footings designed at typical allowable settlements ($0.4\% < s/B < 2\%$), the mean ratio of predicted to measured Q/Q_{L2} increases to about 1.56–1.58.
- (2) The updating of the hyperbolic load-settlement curve with point measurements from full-scale footings using the First-Order Second-Moment Bayesian approach indicated that the updated curve exhibited a softer response in comparison to the original curve.
- (3) The uncertainty in the updated hyperbolic model was also assessed using the Bayesian

- updating process and indicated a significant reduction compared to the prior model. This was reflected in the significant reduction in the COV of the standard deviation of Q/Q_{L2} .
- (4) A quantification of the expected degree of correlation between within-site measurements of load and settlement indicated an average positive correlation coefficient of about 0.26. An investigation of the effect of positive correlation on the updated load-settlement relationship indicated a very minor effect which could be ignored for all practical purposes.
 - (5) An illustrative example using footings with widths of 1.5, 2.5, and 3.0 m indicated that the updated normalized load-settlement relationship generally results in deterministic SLS capacities that are 15% smaller than those obtained using the prior model for a practical allowable settlement of 2.5 cm.
 - (6) The same example was analyzed with the uncertainties in the settlement models and the allowable settlement being considered. The results of the probabilistic analysis indicated average COVs in Q_{SLS} of about 0.24 for the prior normalized load-settlement model and about 0.16 for the updated model. A comparison between these COVs and those obtained for two commonly used SPT-based methods indicated relatively elevated levels of uncertainty in Q_{SLS} for the SPT-based models [COV = 0.67 for Burland and Burbidge (1985) model and 0.79 for the Meyerhof (1965) model].
 - (7) The results of an illustrative SLS reliability analysis that was conducted on the three footings using the prior and updated load-settlement models and the SPT-based models indicated that the updated load-settlement model generally resulted in SLS reliability indices of about 2.5, while the prior model resulted in reliability indices in the order of 1.75. The SPT-based methods exhibited the least reliability with reliability indices in the range of 0.94–1.28. The above results indicate that the SLS design of foundations on sands could require the need for safety factors or resistance/deformation factors if specific target SLS reliability indices are desired in a given design.

It should be mentioned that the reliability analysis that was conducted in this study does not include uncertainty due to spatial variability of soil

properties in its formulation. As a result, the reported reliability indices should be used only for comparative assessments that are aimed at reflecting the effect of the load-settlement model on the SLS probability of failure of the foundation. Moreover, the serviceability limit state that was used as a basis for defining failure in this reliability analysis is based solely on allowable tolerable settlements which were indirectly linked to allowable angular distortions. The analysis does not explicitly use the allowable angular distortion for defining the limit state.

The above limitations could be addressed in future work that will target incorporating spatial variability in the soil properties in the probabilistic assessment of the SLS limit state. This analysis could include an approach that is based on total allowable or tolerable settlements (similar to this paper) and an approach that is based on the concept of tolerable distortions and that would require an assessment of the differential settlements between adjacent foundations (Akbas and Kulhawy 2009c). Moreover, an effort will be conducted to test the performance of a power load-settlement model and compare it with that of the hyperbolic model. This could be done for the case with full load-settlement relationships to be followed with an update using point measurements. Such an analysis could shed light on the comparative performance of the two models (hyperbolic and power) in SLS problems involving full-scale footings on granular soils.

Acknowledgments

The authors would like to acknowledge the University Research Board (URB) at the American University of Beirut for funding this research study.

References

- AASHTO (American Association of State Highway and Transportation Officials). 2004. *LRFD Bridge Design Specifications*. Washington, DC: AASHTO.
- Akbas, S. O. 2007. "Deterministic and Probabilistic Assessment of Settlements of Shallow Foundations in Cohesionless Soils." PhD diss., Cornell University.
- Akbas, S. O., and F. H. Kulhawy. 2009a. "Axial Compression of Footings in Cohesionless Soils. I: Load-Settlement Behavior." *Journal of Geotechnical and Geoenvironmental Engineering* 135 (11): 1562–1574. doi:10.1061/(ASCE)GT.1943-5606.0000135.
- Akbas, S. O., and F. H. Kulhawy. 2009b. "Axial Compression of Footings in Cohesionless Soils. II: Bearing Capacity." *Journal of Geotechnical and Geoenvironmental Engineering* 135 (11): 1575–1582. doi:10.1061/(ASCE)GT.1943-5606.0000136.
- Akbas, S. O., and F. H. Kulhawy. 2009c. "Reliability-Based Design Approach for Differential Settlement of Footings on Cohesionless Soils." *Journal of Geotechnical and Geoenvironmental Engineering* 135 (12): 1779–1788. doi:10.1061/(ASCE)GT.1943-5606.0000127.

- Berardi, R., and R. Lancellotta. 1991. "Stiffness of Granular Soil from Field Performance." *Geotechnique* 41 (1): 149–157. doi:10.1680/geot.1991.41.1.149.
- Briaud, J. L. 2007. "Spread Footings in Sand: Load Settlement Curve Approach." *Journal of Geotechnical and Geoenvironmental Engineering* 133 (8): 905–920. doi:10.1061/(ASCE)1090-0241(2007)133:8(905).
- Burland, J. B., and M. C. Burbidge. 1985. "Settlement of Foundations on Sand and Gravel." *Proceedings – Institution of Civil Engineers*, Part 1 78: 1325–1381.
- Elfass, S., G. Norris, and P. Vimalaraj. 2007. "A Simple Bearing Capacity Equation." *Proceedings of the Geo-Denver 2007: New Peaks in Geotechnics (GSP 171)*, edited by H. W. Olsen, 1–10. Reston, VA: ASCE.
- Fenton, G. A., D. V. Griffiths, and E. Cavers. 2005. "Resistance Factors for Settlement Design." *Canadian Geotechnical Journal* 42: 1422–1436. doi:10.1139/t05-053.
- Gilbert, R. B. 1999. *First-Order Second-Moment Bayesian Method for Data Analysis in Decision Making*. Austin, TX: Geotechnical Engineering Center Report, Department of Civil Engineering, University of Texas at Austin, Texas.
- Jeyapalan, J. K., and R. Boehm. 1986. "Procedure for Predicting Settlements in Sands." *Settlements of Shallow Foundations on Cohesionless Soils: Design and Performance*. Geotechnical Special Publication No. 5, 1–22. Seattle, WA: ASCE.
- Lutenegeger, A. J., and M. T. Adams. 1998. "Bearing Capacity of Footings on Compacted Sand." *Proceedings of the 4th International Conference on Case Histories in Geotechnical Engineering*, 1216–1224, St. Louis, MO.
- Meyerhof, G. G. 1965. "Shallow Foundations." *Journal of Soil Mechanics and Foundations Division, ASCE* 82 (1): 377–393.
- Najjar, S. S., and S. Sadek. 2010. "A Reliability-Based Approach to the Design of Spread Footings on Granular Soil." *Proceedings of GeoFlorida 2010: Advances in Analysis, Modeling and Design*, Geotechnical Special Publication No. 199, 2143–2152. ASCE, West Palm Beach, Florida.
- Schmertmann, J. H., J. P. Hartman, and P. R. Brown. 1978. "Improved Strain Influence Factor Diagrams." *Journal of Soil Mechanics and Foundations Division ASCE*, 104 (8): 1131–1135.
- Shahin, M. A., M. B. Jaksa, and H. R. Maier. 2005. "Neural Network Based Stochastic Design Charts for Settlement Prediction." *Canadian Geotechnical Journal* 42: 110–120. doi:10.1139/t04-096.
- Sivakugan, N., and K. Johnson. 2002. "Probabilistic Design Chart for Settlements of Shallow Foundations in Granular Soils." *Australian Civil Engineering Transactions, CE* 43: 19–24.
- Skempton, A. W., and D. H. MacDonald. 1956. "Allowable Settlement of Buildings." *Proceedings – Institution of Civil Engineers* 5 (3): 727–768.
- Tan, C. K., and J. M. Duncan. 1991. "Settlement of Footings on Sands: Accuracy and Reliability." *Proceedings of the Geotechnical Engineering Congress, Colorado*, Vol. 1, 446–455.
- Terzaghi, K., and R. B. Peck. 1967. *Soil Mechanics in Engineering Practice*. 2nd ed. Washington, DC: John Wiley and Sons.
- Uzielli, M., and P. W. Mayne. 2012. "Load-Displacement Uncertainty of Vertically Loaded Shallow Footings on Sands and Effects on Probabilistic Settlement Estimation." *Georisk: Assessment and Management of Risk for Engineered Systems and Geohazards* 6 (1): 50–69. doi:10.1080/17499518.2011.626333.
- Wang Y., and F. H. Kulhawy. 2008. "Reliability Index for Serviceability Limit State of Building Foundations." *Journal of Geotechnical and Geoenvironmental Engineering, ASCE* 134 (11): 1587–1594. doi:10.1061/(ASCE)1090-0241(2008).
- Zhang, L. M., and A. M. Y. Ng. 2005. "Probabilistic Limiting Tolerable Displacements for Serviceability Limit State Design of Foundations." *Geotechnique* 55 (2): 151–161. doi:10.1680/geot.2005.55.2.151.

Appendix 1

For a footing on granular soil, which is a drained loading problem, the predicted bearing capacity, or predicted tip/base capacity in compression, Q_{tcp} for footings on level ground and without any load inclination or eccentricity is given by the following equation:

$$Q_{tcp} = q_{ult}A_F = Q_{tcp}^v + Q_{tcp}^q \\ = (0.5B\bar{\gamma}N_\gamma\zeta_{\gamma s}\zeta_{\gamma d}\zeta_{\gamma r} + \bar{\gamma}DN_q\zeta_{qs}\zeta_{qd}\zeta_{qr})A_F \quad (A.1)$$

where A_F = footing area; B = footing width; D = footing depth; $\bar{\gamma}$ = effective soil unit weight; N_γ and N_q = bearing capacity factors; $Q_{tcp}^v = Q_{tcp}$ from N_γ portion and $Q_{tcp}^q = Q_{tcp}$ from N_q portion. The factors $\zeta_{\gamma s}$, $\zeta_{\gamma d}$, $\zeta_{\gamma r}$ and ζ_{qs} , ζ_{qd} , ζ_{qr} are correction factors for soil rigidity (r), foundation shape (s), and foundation depth (d). Expressions for all the above parameters could be found in Akbas and Kulhawy (2009b).

Appendix 2

For a dataset, \bar{x} , with an assumed multivariate normal distribution, the natural logarithm of the likelihood function is given by the following (Gilbert 1999):

$$\ln [L(\bar{x}|\bar{\Phi})] \propto -\frac{1}{2} \ln(|C_{\bar{x}}|) - \frac{1}{2} \\ \times (\bar{x} - \bar{\mu}_{\bar{x}})^T C_{\bar{x}}^{-1} (\bar{x} - \bar{\mu}_{\bar{x}}) \quad (B.1)$$

where \bar{x} in the problem under consideration in this study is a vector of all the Q/Q_{L2} measurements which are associated with corresponding measured s/B values. It should be noted that the mean of the measured data $\bar{\mu}_{\bar{x}}$ and the covariance matrix for the measured data \bar{x} are both functions of the probabilistic model parameters, $\bar{\Phi}$.

Appendix 3

For the prior and updated normalized load-settlement relationship, the expected value of Q/Q_{L2} , $E(Q/Q_{L2})$ and the variance of Q/Q_{L2} , $\text{Var}(Q/Q_{L2})$ could be evaluated using a first-order approximation as follows (Gilbert 1999):

$$E(Q/Q_{L2}) = E_{\bar{\Phi}}(\mu_{Q/Q_{L2}|\bar{\Phi}}) \quad (C.1)$$

$$\text{Var}(Q/Q_{L2}) = E_{\bar{\Phi}}(\sigma_{Q/Q_{L2}|\bar{\Phi}})^2 + \text{Var}_{\bar{\Phi}}(\sigma_{Q/Q_{L2}|\bar{\Phi}}) \\ + \text{Var}_{\bar{\Phi}}(E_{Q/Q_{L2}|\bar{\Phi}}) \quad (C.2)$$

where $\mu_{Q/Q_{L2}|\vec{\Phi}}$ and $\sigma_{Q/Q_{L2}|\vec{\Phi}}$ are the mean value and standard deviation of Q/Q_{L2} as indicated in Equation 4 (both are random variables, since they are function of the uncertain model parameters $\vec{\Phi}$), and $E(Q/Q_{L2})$ and $\text{Var}(Q/Q_{L2})$ are the expected mean and variance of Q/Q_{L2} as obtained from the first-order approximation. It should be noted that Equation C.2 indicates that the uncertainty in Q/Q_{L2} arises from two sources: random variability that is modeled by the model parameters, $E_{\vec{\Phi}}(\sigma_{Q/Q_{L2}|\vec{\Phi}})$ and uncertainty in the model parameters themselves, $\text{Var}_{\vec{\Phi}}(\sigma_{Q/Q_{L2}|\vec{\Phi}})$ and $\text{Var}_{\vec{\Phi}}(E_{Q/Q_{L2}|\vec{\Phi}})$. The first and second moments for $\mu_{Q/Q_{L2}|\vec{\Phi}}$ and $\sigma_{Q/Q_{L2}|\vec{\Phi}}$ themselves can be approximated as functions of the first and second moments of the model parameters $\vec{\Phi}$, using first-order Taylor series expansion such that:

$$E_{\vec{\Phi}}(\mu_{Q/Q_{L2}|\vec{\Phi}}) = h_{\mu}(\vec{\mu}_{\vec{\Phi}}) \quad (\text{C.3})$$

$$\text{Var}_{\vec{\Phi}}(E_{Q/Q_{L2}|\vec{\Phi}}) = \left\{ \left. \frac{\delta h_{\mu}}{\delta \vec{\Phi}_i} \right|_{\mu_{\vec{\Phi}}} \right\}^T C_{\vec{\Phi}} \left\{ \left. \frac{\delta h_{\mu}}{\delta \vec{\Phi}_i} \right|_{\mu_{\vec{\Phi}}} \right\} \quad (\text{C.4})$$

$$E_{\vec{\Phi}}(\sigma_{Q/Q_{L2}|\vec{\Phi}}) = h_{\sigma}(\vec{\mu}_{\vec{\Phi}}) \quad (\text{C.5})$$

$$\text{Var}_{\vec{\Phi}}(\sigma_{Q/Q_{L2}|\vec{\Phi}}) = \left\{ \left. \frac{\delta h_{\sigma}}{\delta \vec{\Phi}_i} \right|_{\mu_{\vec{\Phi}}} \right\}^T C_{\vec{\Phi}} \left\{ \left. \frac{\delta h_{\sigma}}{\delta \vec{\Phi}_i} \right|_{\mu_{\vec{\Phi}}} \right\} \quad (\text{C.6})$$

where $\left\{ \left. \frac{\delta h_{\mu}}{\delta \vec{\Phi}_i} \right|_{\mu_{\vec{\Phi}}} \right\}$ and $\left\{ \left. \frac{\delta h_{\sigma}}{\delta \vec{\Phi}_i} \right|_{\mu_{\vec{\Phi}}} \right\}$ are vectors containing the partial derivatives of $h_{\mu}(\vec{\Phi})$ and $h_{\sigma}(\vec{\Phi})$, respectively, evaluated at the mean values of the model parameters, and $h_{\mu}(\vec{\Phi})$ and $h_{\sigma}(\vec{\Phi})$ are the expressions of the probabilistic model of the $\mu_{Q/Q_{L2}}$ and $\sigma_{Q/Q_{L2}}$, respectively, as reflected in Equation 4.

Finally, for the case where the allowable tolerable settlement is included in the analysis as an uncertain parameter, all the previous equations could still be utilized with the incorporation of s/B as an additional uncertain parameter (Φ_4) in Equation 4. With regard to the two SPT-based models, the two uncertain parameters that were included in the analysis are the model uncertainty λ and the allowable settlement δ_{all} . A first-order approximation was also used to evaluate the mean and standard deviation of Q_{SLS} , such that:

$$\mu_{Q_{\text{SLS}}} = \frac{N_{60}(B + 0.3)^2}{2.12 \left(1 - \frac{D_f}{4B}\right)} \mu_{\delta_{\text{all}}} \text{ for } B > 1.22 \text{ m} \quad (\text{C.7})$$

$$\mu_{Q_{\text{SLS}}} = \frac{B^{1.3} (N_{60})^{1.4}}{1.71 \mu_{\lambda}} \mu_{\delta_{\text{all}}} + \gamma D_f B^2 \quad (\text{C.8})$$

$$\sigma_{Q_{\text{SLS}}} = \sqrt{\left(\frac{\delta Q_{\text{SLS}}}{\delta \lambda} \right)^2 (\sigma_{\lambda})^2 + \left(\frac{\delta Q_{\text{SLS}}}{\delta \delta_{\text{all}}} \right)^2 (\sigma_{\delta_{\text{all}}})^2} \quad (\text{C.9})$$

It should be noted that Equation C.9 applied to the two SPT-based models.